

Sensorless Maximum Power Point Tracking control for Wind Energy Conversion System using DFIG

L. Jerbi, L. Krichen and A. Ouali

Advanced Control and Energy Management research unit ENIS, 3038 Sfax, Tunisia.

Lilia.Jerbi@issatgb.rnu.tn
lotfi.krichen@enis.rnu.tn
abderrazak.ouali@enis.rnu.tn

Abstract: This paper proposes a variable speed Wind Energy Conversion System (WECS) using Doubly Fed Induction Generator (DFIG). The vector control of the DFIG is achieved according to the generator speed in order to maximize the wind power capture (MPPT). The proposed control scheme is ensured without mechanical and wind speed sensors from the aspect of reliability and increase in cost. The system drive considers a reduced state model of the DFIG with an oriented stator flux. An adaptive observer has been developed to the considered structure in which the electrical sizes are estimated from the stator currents measure and the shaft speed is adjusted optimally through an adaptation law derived from Lyapunov stability theory. An extended Luenberger observer is also applied to a linear mechanical state model to estimate the wind torque. This system design provides wind speed estimation, which is required in the maximization control algorithm. The simulation results show the effectiveness of the considered DFIG drive.

Index Terms: WECS, DFIG, MPPT, Adaptive Observer, Sensorless Control, Lyapunov stability theory, Extended Luenberger Observer.

1. Introduction:

The DFIG has been a competitive choice in the wind power generation at variable speed [1]-[3]. The structure which including power converters on the rotor side provides a high degree of controllability and permits to achieve maximum efficiency at all wind velocities. In order to ensure MPPT control, the DFIG vector control is needed. The control scheme of the machine requires thus, rotor speed and wind velocity for optimal operating. Therefore the sensors use to measure these previous sizes involves increase in installation complexity and cost. For this effect, sensorless drive is desired and becomes an important topic for several WECS. From this point of view, several researches have considered sensorless machine drive. In [4], a Permanent Magnet Synchronous generator (PMSG) is controlled by the loss-minimization control with an MPPT algorithm below the base speed, which corresponds to low and medium wind speed. Above the base speed corresponding to high wind speed region, the current and voltage limited maximum output control is applied, where the current vector is determined by the simple low-order polynomials with respect to the generator speed. The proposed output maximization control is achieved without mechanical sensors such as

wind speed sensor and position sensor and its effectiveness is evaluated for laboratory experiment. The authors [5] propose also a sensorless MPPT control of wind generator using PMSG. The rotor position is estimated from flux linkages using the first-order lag compensator. The rotor speed and wind velocity are estimated by using a full-order observer. The optimal rotor speed is therefore determined using the estimated value obtained. In addition, improving the efficiency of the wind generator is performed by optimizing d-axis current using the Powell method [6]. Moreover, a simple position-sensorless method for rotor side field oriented control of the DFIG is adopted in [7]. The algorithm design which is based on axis transformation permits to reduce the dependence of machine parameters. It can be started on the fly without the knowledge of the initial rotor position and ensure a stability operating at synchronous speed corresponding to zero rotor frequency. This makes consequently suitable for variable speed constant frequency operations largely required in WECS. Whereas, the structure explored in [8] suggests a sensorless decoupled P-Q control of the DFIG using a γ - δ axes tracker which applies Phase Lock Loop principles. Reference [9], presents an analysis of a Model Reference Adaptive System (MRAS) observer for the sensorless control of a standalone DFIG. The analysis allows the formal design of the MRAS observer of given dynamics and further allows the prediction of rotor position estimation errors under parameter mismatch. The estimation structure uses in fact two models: voltage model and current model. The first one permits to obtain the reference of the stator flux, while the former is devoted to estimate it by adjusting the estimated rotational speed through a PI controller.

This paper deals with a sensorless MPPT control for WECS using DFIG based on adaptive observer [10]-[12]. The vector control of the machine is ensured without wind and mechanical sensors by considering a reduced state model with an oriented stator flux. The observer design permits to estimate the rotor currents from voltages and stator currents measurement. The rotor speed is obtained via an adaptation law derived from Lyapunov stability theory. An additional extended Luenberger observer is moreover addressed to estimate the aerodynamic torque which gives estimation to the wind speed. The DFIG model and the adaptive observer design are first defined.

Secondly, the sensorless vector control of the wind generator based on rotor currents estimation is described. The estimation of the aerodynamic torque and the wind speed are then considered. Finally, the effectiveness of the proposed observer is shown through simulation results.

2. DFIG model:

The proposed WECS as it is shown in figure1 consists of a DFIG driven by a wind turbine and controlled on the rotor side via power converters. The machine equations written in a synchronously rotating d-q reference frame with oriented stator flux are [13]:

$$\begin{cases} \frac{d}{dt} X = A(\Omega_{mec}) X + B_r V_r + B_g V_g \\ I_s = C X \\ \frac{d}{dt} \Omega_{mec} = (C_{aero} - C_{em}) / J \end{cases} \quad (1)$$

where:

$$X = \begin{bmatrix} i_{rd} & i_{rq} & \phi_{sd} \end{bmatrix}^T, V_r = \begin{bmatrix} v_{rd} & v_{rq} \end{bmatrix}^T; \\ V_g = \begin{bmatrix} V_{gd} & V_{gq} \end{bmatrix}^T; I_s = \begin{bmatrix} i_{sd} & i_{sq} \end{bmatrix}^T$$

$$A(\Omega_{mec}) = \begin{bmatrix} -\frac{(r_r + \frac{m^2 r_s}{l_s^2})}{\sigma l_r} & (\omega_s - \Omega_{mec}) & \frac{m r_s}{\sigma l_r l_s^2} \\ -(\omega_s - \Omega_{mec}) & -\frac{r_r}{\sigma l_r} & -(\omega_s - \Omega_{mec}) \frac{m}{\sigma l_r l_s} \\ \frac{m r_s}{l_s} & 0 & -\frac{r_s}{l_s} \end{bmatrix}$$

$$B_r = \begin{bmatrix} \frac{1}{\sigma l_r} & 0 & 0 \\ 0 & \frac{1}{\sigma l_r} & 0 \end{bmatrix}^T, B_g = \begin{bmatrix} \frac{m}{\sigma l_r l_s} & 0 & -1 \\ 0 & 0 & 0 \end{bmatrix}^T, \\ C = \begin{bmatrix} -\frac{m}{l_s} & 0 & \frac{1}{l_s} \\ 0 & -\frac{m}{l_s} & 0 \end{bmatrix}$$

with:

i_{rd} and i_{rq} are the d and q components of the rotor current, respectively.

i_{sd} and i_{sq} are the d and q components of the stator current, respectively.

ϕ_{sd} is the d component of the stator flux.

v_{rd} and v_{rq} are the d and q components of the rotor voltage, respectively.

V_{gd} and V_{gq} are the d and q components of the grid voltage, respectively.

ω_s and Ω_{mec} are the synchronous pulsation and the mechanical speed, respectively.

r_s and r_r are the stator and rotor resistors, respectively.

l_s , l_r and m are the stator, the rotor and the mutual inductances, respectively.

σ is a leakage coefficient such as $\sigma = 1 - \frac{m^2}{l_s l_r}$.

J is the wind generator inertia.

C_{em} and C_{aero} are the electromagnetic and wind torques, respectively defined by :

$$C_{em} = \frac{m}{l_s} i_{rq} \phi_{sd} \quad (2)$$

and

$$C_{aero} = \frac{1}{2} \frac{C_p(\lambda) \rho \pi R^3 v^2}{\lambda G} \quad (3)$$

with:

C_p is the power coefficient, ρ is the air density, R is the blade radius, v is the wind speed, G is the gear ratio and λ is the specific speed.

3. Sensorless MPPT of the DFIG:

To extract the maximum of wind power, the DFIG control is ensured by the converter1 (Conv1) in the rotor side. A vector control of the rotor currents is thus necessary to fix the rotor voltages ensuring an optimal operating. Relating to the DFIG model given by (1), the control laws are elaborated as following [14]:

$$\begin{cases} v_{rd} = \sigma l_r (v_{rd0} + (\omega_s - \Omega_{mec}) (i_{rq0} - i_{rq}) \\ \quad + (k_1 + \frac{k_2}{p}) (i_{rd0} - i_{rd})) \\ v_{rq} = \sigma l_r (v_{rq0} - (\omega_s - \Omega_{mec}) (i_{rd0} - i_{rd}) \\ \quad + (k'_1 + \frac{k'_2}{p}) (i_{rq0} - i_{rq})) \end{cases} \quad (4)$$

where:

k_1 , k_2 , k'_1 and k'_2 are the regulators parameters.

The reference values of the rotor currents are determined by the computation of the optimal balance point. An Artificial Neural Network (ANN) with Radial Basic Functions (RBF) provides this optimal steady state according to the random wind speed and the desired reactive power injected into grid on the stator side. Consequently, the control scheme requires mechanical speed and wind velocity measures. Sensorless vector control will be significant in this case to reduce the installation cost and limit the measurements only on the stator size coupled to the power electric system. Thus, the

rotor currents and the mechanical speed in the control laws (4) will be replaced by the estimated one calculated via an adaptive observer so that we obtain:

$$\begin{cases} v_{rd} = \sigma l_r (v_{rd0} + (\omega_s - \hat{\Omega}_{mec}) (i_{rq0} - \hat{i}_{rq}) \\ \quad + (k_1 + \frac{k_2}{p}) (i_{rd0} - \hat{i}_{rd})) \\ v_{rq} = \sigma l_r (v_{rq0} - (\omega_s - \hat{\Omega}_{mec}) (i_{rd0} - \hat{i}_{rd}) \\ \quad + (k_1' + \frac{k_2'}{p}) (i_{rq0} - \hat{i}_{rq})) \end{cases} \quad (5)$$

The proposed sensorless control is accomplished without mechanical and wind speed sensors. It is based on adaptive and Extended Luenberger observer as is shown in figure1.

3. Adaptive observer design:

Relating to the state model given by (1), the observer structure considers two schemes. The first one estimates the electric variables corresponding to the rotor currents and the stator flux. The second permits to adjust the rotor speed through an adaptation law. Therefore, the observer can be written as [15]:

$$\frac{d}{dt} \hat{X} = A(\hat{\Omega}_{mec}) \hat{X} + B_r V_r + B_g V_g + L(I_s - \hat{I}_s) \quad (6)$$

where $\hat{\cdot}$ means estimated values.

L is the observer gain defined by :

$$L = \begin{bmatrix} l_1 & l_2 & l_3 \\ l_4 & l_5 & l_6 \end{bmatrix}^T$$

We indicate e the estimation error such as:

$$e = X - \hat{X} = \begin{bmatrix} e_{ird} & e_{irq} & e_{\phi_{sd}} \end{bmatrix}^T \quad (8)$$

where:

$$e_{i_{rd}} = i_{rd} - \hat{i}_{rd}, \quad e_{i_{rq}} = i_{rq} - \hat{i}_{rq} \quad \text{and} \quad e_{\phi_{sd}} = \phi_{sd} - \hat{\phi}_{sd}$$

The estimation error dynamic, is:

$$\dot{e} = (A(\hat{\Omega}_{mec}) - LC) e + \Delta A X \quad (9)$$

with: $\Delta A = A(\hat{\Omega}_{mec}) - A(\hat{\Omega}_{mec}^*)$

To ensure the observer stability, the observer gain L is chosen so that $(A(\hat{\Omega}_{mec}) - LC)$ was stable. The estimation error will converge asymptotically to zero if we obtain:

$$\lim_{t \rightarrow \infty} \hat{\Omega}_{mec} = \Omega_{mec} \quad (10)$$

and

$$\lim_{t \rightarrow \infty} \hat{X} = X \quad (11)$$

4. Speed adaptation law:

To achieve the speed adaptation law, we define a Lyapunov function as:

$$V(e, \Delta\Omega) = e^T P e + \alpha (\Delta\Omega)^2 \quad (12)$$

(7) where: $\Delta\Omega = \Omega_{mec} - \hat{\Omega}_{mec}^*$ is the speed variation, α is a positive coefficient, P is a positive symmetrical matrix

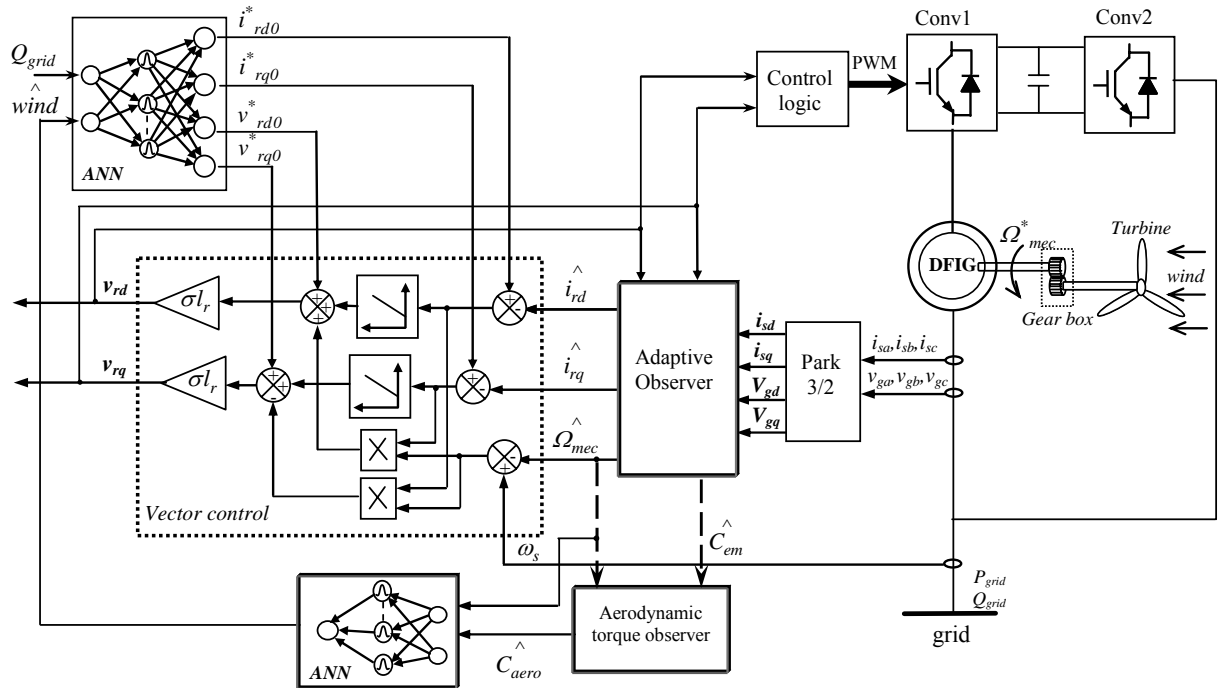


Figure 1 Sensorless vector control scheme of the DFIG

verifying the Lyapunov equation expressed by :

$$(A(\hat{\Omega}_{mec}) - LC)^T P + P (A(\hat{\Omega}_{mec}) - LC) = -Q \quad (13)$$

with Q is a symmetric positive definite matrix.

The derivative of the Lyapunov function gives:

$$\begin{aligned} \dot{V} = e^T & \left[(A(\hat{\Omega}_{mec}) - LC)^T P + P (A(\hat{\Omega}_{mec}) - LC) e \right] \\ & + 2 \hat{X}^T \Delta A^T P e - 2 \alpha \Delta \Omega \frac{d}{dt} \hat{\Omega}_{mec} \end{aligned} \quad (14)$$

The system stability is ensured when \dot{V} is negative. This makes consequently, the first term in (14) to be negative and leads to annul the second one. So, we obtain:

$$e^T \left[(A(\hat{\Omega}_{mec}) - LC)^T P + P (A(\hat{\Omega}_{mec}) - LC) e \right] < 0 \quad (15)$$

and :

$$2 \hat{X}^T \Delta A^T P e - 2 \alpha \Delta \Omega \frac{d}{dt} \hat{\Omega}_{mec} = 0 \quad (16)$$

Expression (15) is negative and verifies the Lyapunov equation. Expression (16) can be also written as:

$$\alpha \frac{d}{dt} \hat{\Omega}_{mec} = \hat{X}^T H^T P V_1 - \frac{l_{sl}}{m} \hat{X}^T H^T P V_2 \quad (17)$$

with:

$$H = \begin{bmatrix} 0 & -1 & 0 \\ 1 & 0 & \frac{m}{\sigma l_r l_{sl}} \\ 0 & 0 & 0 \end{bmatrix}, \quad V_1 = (\phi_{sd} - \hat{\phi}_{sd}) \begin{bmatrix} 1 & 0 & 1 \end{bmatrix}^T,$$

$$V_2 = \begin{bmatrix} i_{sd} - \hat{i}_{sd} & i_{sq} - \hat{i}_{sq} & 0 \end{bmatrix}^T$$

This last equation illustrates that the speed adaptation law depends on two expressions. One is relating to (X, \hat{X}) which can be assumed as disturbance, whereas the other depends on $(\hat{X}, I_s - \hat{I}_s)$.

By supposing the weak variations of the stator flux, the adaptation mechanism of the mechanical speed is deduced as following:

$$\frac{d}{dt} \hat{\Omega}_{mec} = -\frac{l_s}{\alpha m} \begin{bmatrix} -\alpha_1 \hat{i}_{rq} (i_{sd} - \hat{i}_{sd}) + \\ \alpha_2 \hat{i}_{rd} (i_{sq} - \hat{i}_{sq}) \end{bmatrix} \quad (18)$$

where α_1 and α_2 are adjustable gains relating to the P matrix.

Figure 2 shows a block diagram of the proposed speed adaptation law. The speed estimation is obtained from the product of the estimation error in stator current by the estimated rotor current associated to variable gains. Then a PI controller with an appropriate proportional and integration gain regulates the estimated speed so that the speed estimation error will be null.

5. Aerodynamic torque observer:

As it was previously indicated, the electromagnetic torque is estimated from the adaptive observer by the following expression:

$$\hat{C}_{em} = \frac{m}{l_s} \hat{i}_{rq} \hat{\phi}_{sd} \quad (19)$$

The DFIG state model can be augmented by the aerodynamic torque assumed constant and varies slowly. So, the hypothesis of:

$$\frac{d}{dt} C_{aero} = 0 \quad (20)$$

permits to obtain the following state model defined as:

$$\begin{cases} \frac{d}{dt} X_t = A_t X_t + B_t C_{em} \\ \hat{\Omega}_{mec} = C_t X_t \end{cases} \quad (21)$$

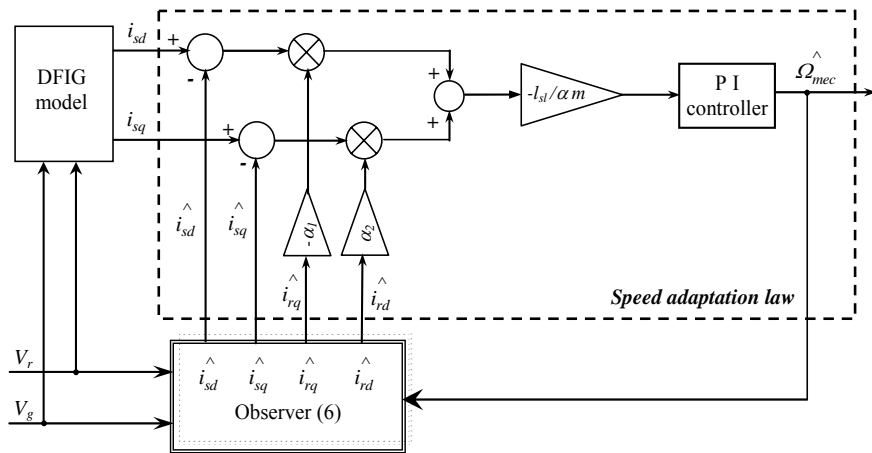


Figure 2 Configuration of the proposed speed adaptation law

where:

$$X_t = \begin{bmatrix} \Omega_{mec} \\ C_{aero} \end{bmatrix}, \quad A_t = \begin{bmatrix} 0 & \frac{1}{J} \\ 0 & 0 \end{bmatrix},$$

$$B_t = \begin{bmatrix} -\frac{1}{J} & 0 \end{bmatrix}^T, \quad C_t = \begin{bmatrix} 1 & 0 \end{bmatrix}$$

The extended Luenberger observer associated to the mechanical state model defined by (21) is:

$$\frac{d}{dt} \hat{X}_t = A_t \hat{X}_t + B_t C_{em} + G (\Omega_{mec} - \hat{\Omega}_{mec}) \quad (22)$$

with, G is the observer gain such as $G = [g_1 \ g_2]^T$

The observer stability is ensured by a suitable choice of the gain G so that $(A_t - GC)$ was stable.

Expression (22) shows the existence of C_{em} and Ω_{mec} which are not accessible in the proposed control algorithm, for that we substitute them by the estimated values \hat{C}_{em} and $\hat{\Omega}_{mec}$ provided by the adaptive observer. Figure 3 shows a block scheme of the extended Luenberger observer applied.

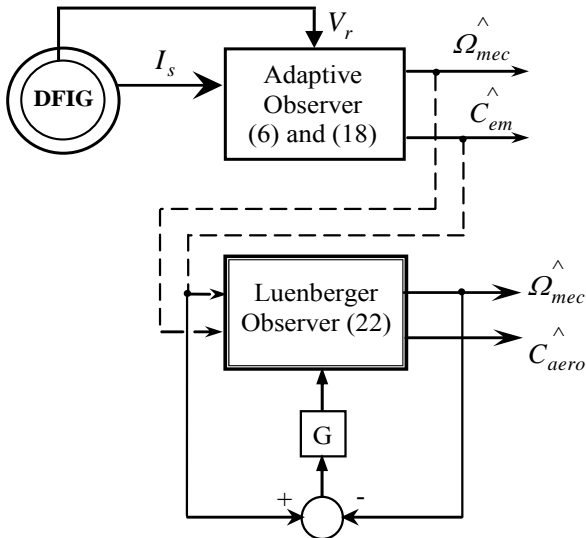


Figure 3 Block diagram of Luenberger observer applied

6. Wind speed estimation:

The wind speed is required to ensure an optimal operating of the DFIG [14]. However, in practice a precise measure of the wind speed is difficult to produce because of the wind sensor is located behind the turbine rotor. Moreover, a wrong measure in the wind speed leads certainly to degradation in the power capture. For these reasons, it is suitable to ensure the wind generator control without wind sensor which has been an important topic addressed by several researchers [6]-[7]. The idea proposed here permits to estimate directly the wind speed

from the optimal wind torque and the speed generator previously determined. In fact by knowing, $\hat{\Omega}_{mec}$ and \hat{C}_{aero} which are provided by the adaptive observer and the extended Luenberger observer, respectively, an Artificial Neuronal Network (ANN) gives an approximation of the wind speed needed in the MPPT control scheme.

7. Simulation results and interpretations:

All simulations are run with the 100s duration with the same wind variation by chosen a null reactive power injected into grid on the stator side $Q_{grid} = 0$. The comparison between the real rotor currents and the stator flux of the DFIG associated to sensors with the estimated one resulting from the adaptive observer are shown in figure 4 and 5.

The plots shown in figure 6 correspond to the real and the estimated mechanical speed provided by the speed adaptation law. The curves illustrate the effectiveness of the adaptation loop to adjust the mechanical speed optimally.

The curves given by figure 7 illustrate the convergence of the measured stator currents to the estimated one required in the control loop of the rotor current. This proves the observer performance in term of error estimation.

The estimated electromagnetic torque given by figure 8 and the aerodynamic one shown in figure 9 permit to approximate the wind speed with minimum convergence error as is seen in figure 10.

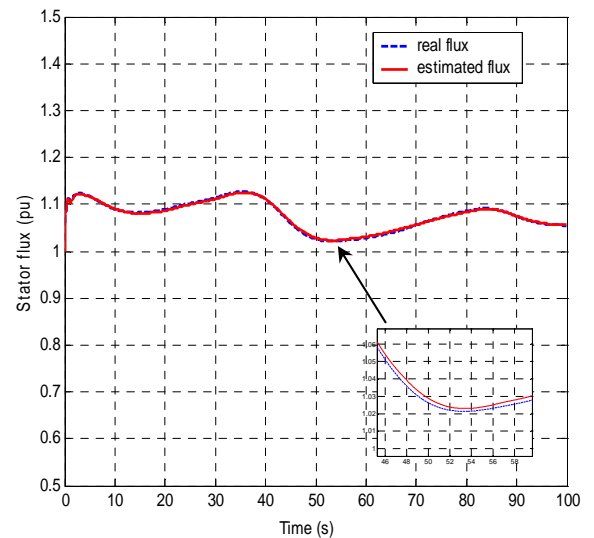


Figure 4 Stator flux curves (ϕ_{sd} and $\hat{\phi}_{sd}$)

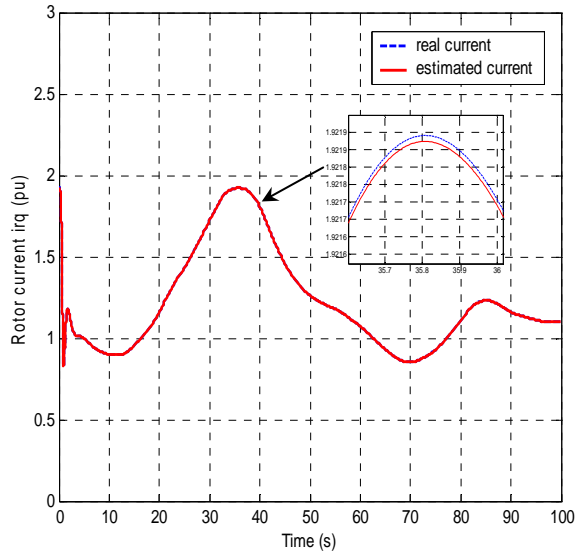
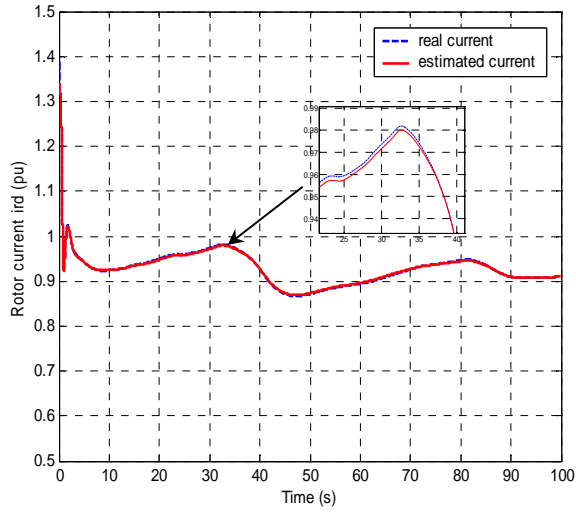


Figure 5 Rotor currents curves (i_{rd} , \hat{i}_{rd} , i_{rq} and \hat{i}_{rq})

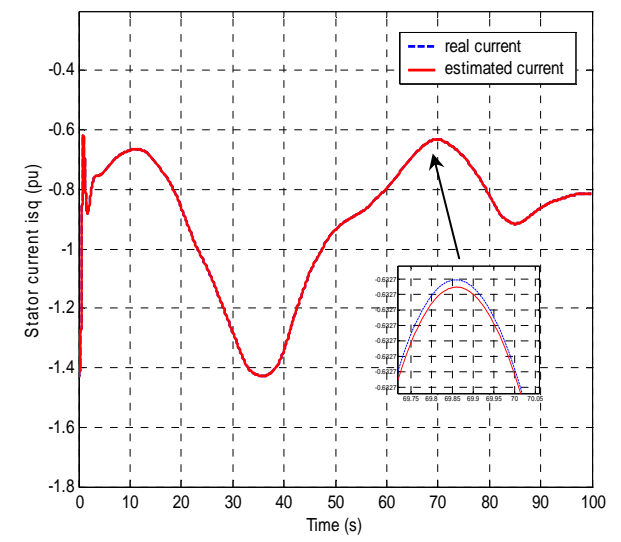
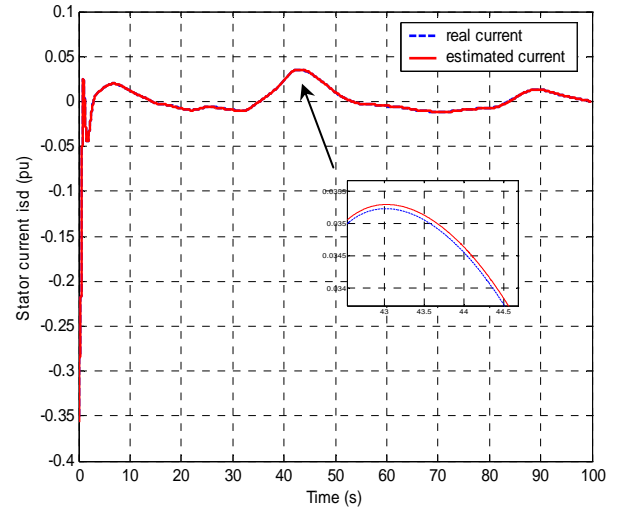


Figure. 7. Stator currents curves (i_{sd} , \hat{i}_{sd} , i_{sq} and \hat{i}_{sq})

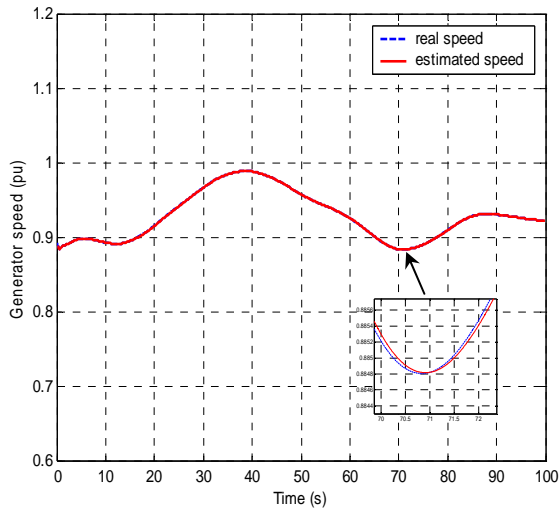


Figure 6 Generator speed curves (Ω_{mec} and $\hat{\Omega}_{mec}$)

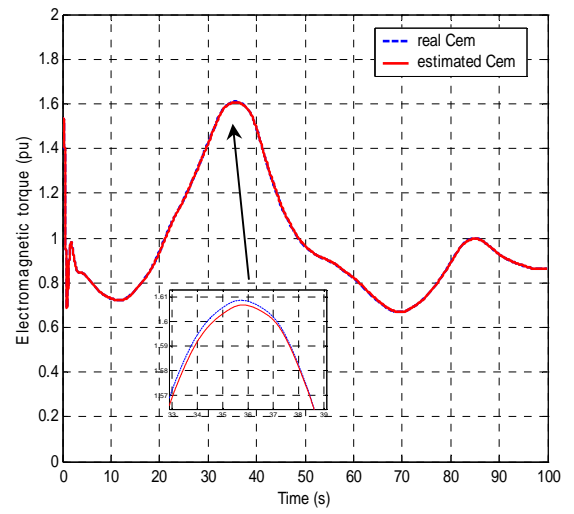


Figure 8. Electromagnetic torque curves (C_{em} and \hat{C}_{em})

APPENDIX

All the parameters are given in pert unit (*pu*)

A. DFIG

Nominal Power 100KW
 Base voltage 600V
 Stator resistor $r_s = 0$
 Rotor resistor $r_r = 0.0043$
 Stator inductance $l_s = 1.59$
 Rotor inductance $l_r = 1.317$
 Mutual inductance $m = 1.159$
 Inertia $J_{DFIG} = 1000$

B. Wind turbine

Gear box $G = 70$
 Number of blades 3
 Blade radius 12m

C. Grid

Voltage grid $V_g = 1$
 Synchronous speed $\omega_s = 1$

ACKNOWLEDGMENT

This study, achieved in the research unit “Advanced Control and Energy Management” ACES of the National School of Engineering of Sfax, enters in the setting of the research project federated “Systèmes Eoliens” sustained by the State Secretariat to the Scientific Research and Technology and coordinated by the National Management Energy Agency. We thank the ENIS, the SERST and the ANME.

REFERENCES

- [1] H.Akagi, H.Sato, “Control and performance of a doubly-fed induction machine intended for a flywheel energy storage system”, IEEE Trans. On Power Electronics, Vol.17, Issue 1, Jan.2002, Page(s): 109-116.
- [2] Ledesma, J.Usaola, “Doubly Fed Induction Generator Model for Transient Stability Analysis”, IEEE Trans. On Energy Conversion, Vol. 20, No. 2, JUNE 2005.
- [3] Rajib Datta and V. T. Ranganathan, “Variable-Speed Wind Power Generation Using Doubly Fed Wound Rotor Induction Machine—A Comparison With Alternative Schemes”, IEEE Trans. Energy, Conversion, vol17, pp. 414-421, September 2002.
- [4] S. Moriimoto, H. Nakayama, M. Sanada and Y.Takeda, “Sensorless Output Maximization Control for Variable-Speed Wind Generation System Using IPMSG”, IEEE Trans. On industry Applications, vol. 41, no 1, January/ February 2005, pp. 60-67.
- [5] T. Senjyu, S. Tamaki, E. Muhando, N. Urasaki, H. Kinjo, T. Funabashi, H. Fujita and H. Sekine, “Wind velocity and rotor position sensorless maximum power point tracking control for wind generation system”,

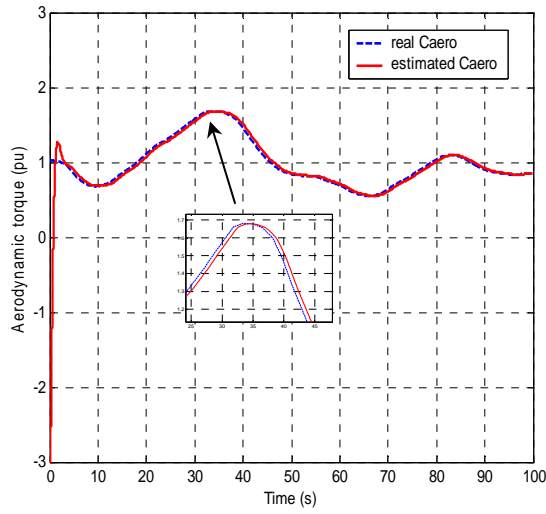


Figure 9 Aerodynamic torque curves (C_{aero} and \hat{C}_{aero})

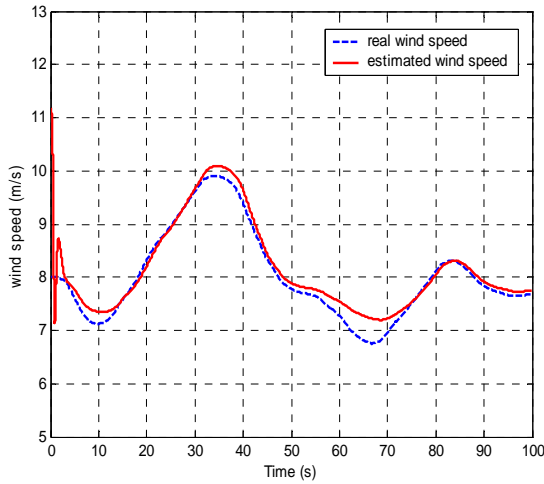


Figure 10 Wind speed curves ($wind$ and \hat{wind})

8. Conclusion:

The sensorless MPPT control of the DFIG is proposed in this paper. The vector control of the rotor current is achieved without mechanical and wind speed sensors. The control algorithm of the proposed WECS considers an adaptive observer which estimates the electric variables of the machine and an adaptation law derived from Lyapunov stability theory to adjust the generator speed. An extended Luenberger observer was also investigated to estimate the wind torque and permits consequently to approximate the wind speed. The control scheme performances are illustrated by simulation results.

Electric Power Systems Research, Renewable Energy 31 (2006) 1764-1775.

[6] T. Senjyu, T. Hamano, N. Urasaki, K. Uezato, T. Funabashi, H. Fujita, "Maximum power point tracking control for wind power generating system using permanent magnet synchronous generator", Trans IEE Japan 2002; 122-B (12): 1403-9.

[7] R.Datta and V.T.Ranganathan, "A Simple Position-Sensorless Algorithm for Rotor-Side Field-Oriented Control of Wound-Rotor Induction Machine", *IEEE, Trans, On.Indust.Electronics*, vol.48, No4, pp786-793, August 2001.

[8] B. Shen, B. Teck Ooi, "Novel Sensorless Decoupled P-Q Control of Doubly-Fed Induction Generator (DFIG) based on Phase Locking to γ - δ Frame", IEEE 2005, pp.2670-2675.

[9] R. Cárdenas, R. Peña, J. Proboste, G. Asher and J. Clare, "MRAS Observer for Sensorless Control of Standalone Doubly Fed Induction Generators", IEEE Trans. on Energy, conversion, vol.19, No2, June 2004.

[10] H. Kubota, I. Sato, Y. Tamura, K. Matsuse, H. Ohta, and Y. Hori, "Regenerating-Mode Low-Speed Operation of Sensorless Induction Motor Drive With Adaptive Observer", *IEEE Trans. on Indust. Applications*, vol.38, No. 4, pp. 1081-1086 July/August 2002.

[11] N. Bensiali, C. Chaigne, S. Tnani, E. Etienl and G. Champenois, "Optimal Observer Design for Sensorless Control of Induction Motor in Regenerating-Mode", *SPEEDAM 2006 International Symposium on Power Electronics, Electrical Drives, Automation and Motion*.

[12] Hinkkanen and J. Luomi, "Stabilization of Regenerating-Mode Operation in Sensorless Induction Motor Drives by Full-Order Flux Observer Design", *IEEE Trans. On Indust. Electronics*, vol.51, No. 6, pp 1318-1328, December 2004.

[13] L. Jerbi, and A. Ouali "Control of a wind generator with wound rotor coupled to the power electric system", CERE 2005, 24-26 March 2005, Sousse, Tunisia.

[14] L. Jerbi, L. Krichen, A. Ouali, "Optimal control of variable wind speed generator based on artificial neural networks", *Archives of Control Sciences*, Vol.16 (LII), no.4, 2006, pp 363-373.

[15] H. Kubota, I. Sato, Y. Tamura, K. Matsuse, Hi. Ohta, Y. Hori, « Regenerating-Mode Low-Speed Operation of Sensorless Induction Motor Drive with Adaptive Observer » IEEE Transactions on Industry Applications, vol. 38, No.4, pp.1081-1086, July/August. 2002.